CHAPTER 7. DETERMINISTIC FORMATION MISSION DESIGN PROBLEM

In this chapter, to show the effectiveness of the methodology described in Chapter 4 in solving the formation mission design problem in the absence of uncertainties, the results of three different numerical experiments will be described. All the experiments involve transoceanic eastbound flights operated by Airbus 330-200 aircraft. In the first experiment, a two-aircraft formation mission design problem is solved, in which one flight's departure time is free. Then, the optimal solution of this problem has been assumed as the baseline case for the next experiment, in which different delays in the departure times of both flights have been considered. Finally, a three-aircraft formation mission design problem is solved, in which different fuel savings schemes have been considered. For each experiment, a detailed description of the results is given together with a comparison with the results obtained in solo flights.

7.1. General description of the experiments

The following numerical experiments have been carried out:

- Experiment A: Two-aircraft transoceanic mission design with one flight's departure time free.
- Experiment B: Two-aircraft transoceanic mission design with delays in the departure times.
- Experiment C: Three-aircraft transoceanic mission design with different fuel savings schemes.

All the experiments involve transoceanic eastbound flights. Wind data from the ERAINTERIM reanalysis database has been used. As mentioned above, in this study only the cruise phase has been modeled, the rest of the flight phases are neglected. Thus, the initial and final cruise phase locations of the cruise phase of the flights have been assumed to be the latitudes and longitudes of the departure and arrival airports of each flight at cruise altitude. Airbus A330-200 aircraft BADA models have been considered for each flight. The initial mass of each aircraft is assigned as well as the initial and final velocities, which have been set at typical cruise values for the selected aircraft models. The initial heading angle is set to the initial heading angle of the orthodromic path between the initial and final locations of each flight. Arrival times are left free and a constraint on the maximum temporal deviation from the scheduled arrival time of 45 minutes has been introduced for each flight. The time and fuel burn weighting parameters, α_t and α_f, in the objective functional have been set to 0.3 and 0.7, respectively, based on the CI definition, as explained in Section 3.4.

The numerical experiments have been conducted on a 3.6 GHz Intel Core i9 computer with 32 GB RAM. The computational times reported in this section include both the time required to generate the warm-start solution and the time to find the optimal solution of the problem. The warm-start solution is a feasible solution of the problem generated by the NLP solver from initial guesses of the solution. The initial guesses for the latitude, the longitude and the heading angle have been generated using the orthodromic between departure and arrival locations of each flight. Typical cruise velocity and fuel consumption of the aircraft model selected have been used to generate the initial guesses of the velocity and the mass of each aircraft during the flight, respectively.

7.2. Experiment A: Two-aircraft transoceanic mission design with one flight's departure time free

7.2.1. Description of the experiment

Experiment A involves two transoceanic eastbound flights, Flight 1 and Flight 2, with given fuel savings for the trailing aircraft and boundary values of the state variables. Flight 1 and Flight 2 are operated by Aircraft 1 and Aircraft 2, respectively. In the SOCP stated to solve the mission design problem, the departure time of Flight 1 is fixed, whereas the departure time of Flight 2 is left free. In case of formation, Aircraft 1 will be the trailing one and Aircraft 2 will be the leader. Solving this problem entails to decide which mode of flight, i.e. formation or solo flight, is optimal, the optimal trajectories of the aircraft and the optimal departure time of Flight 2. Additionally, in case of formation flight, the rendezvous and splitting locations and times must also be determined. To check the optimality of the obtained solution, a comparison between formation flight and solo flight results has been carried out.

The two transoceanic flights considered in this experiment have the following departure and arrival locations:

- Flight 1: New York (JFK) - Madrid (MAD).
- Flight 2: Montreal (YUL) - London (LHR).

The fuel burn savings for the trailing aircraft is set to 10%. The departure time of Flight 1 has been set to 10:15. The boundary conditions for the state variables of each aircraft are listed in Table 7.1.

Table 7.1. Experiment A: Boundary conditions.

Symbol	Units	Flight 1	Flight 2
ϕ_I	[deg]	40.64	45.47
ϕ_F	[deg]	40.48	51.47
λ_I	[deg]	−73.78	−73.74
λ_F	[deg]	−3.57	−0.45
χ_I	[deg]	66.51	55.70
V_I	[m/s]	240	240
V_F	[m/s]	220	220
m_I	[kg]	220000	215 000

As mentioned above, the formation configuration is selected in advance. In case of formation flight, Aircraft 1, associated to Flight 1, is forced to be the trailing aircraft. Hence, Aircraft 2, associated to Flight 2, will be the leader one.

7.2.2. Results

Optimal routes

In the optimal solution, formation flight has been selected as the optimal solution and the obtained optimal departure time for Flight 2 has been 10:50, 35 minutes after the departure of Flight 1. The obtained optimal formation flight routes are represented in Fig. 7.1, together with the solo flight routes and the wind field. In this figure, dashed lines are used to plot solo flight routes and solid lines are used to represent formation flight routes. Green and blue lines represent Flight 1 and Flight 2, respectively.

Flight 1 starts 35 minutes before Flight 2, and due to this difference in the departure times, the optimal solution implies a large initial detour of Flight 1 with respect to solo flight, in order to join Flight 2 as soon as possible, thereby, the rendezvous point is very close to the departure location of Flight 2.

Optimal state and control variables

The corresponding state and control variables are represented in Fig. 7.2 and Fig. 7.3, respectively. For a better understanding of these figures, the portions of the plots of the variables that correspond to formation flight have been represented on a grey background. It can be observed that the heading angle and the Mach number of both aircraft are the same during the formation, as opposed to the mass flow rate which is different for each aircraft.

Fig. 7.1. Experiment A: Solo and formation flight routes.

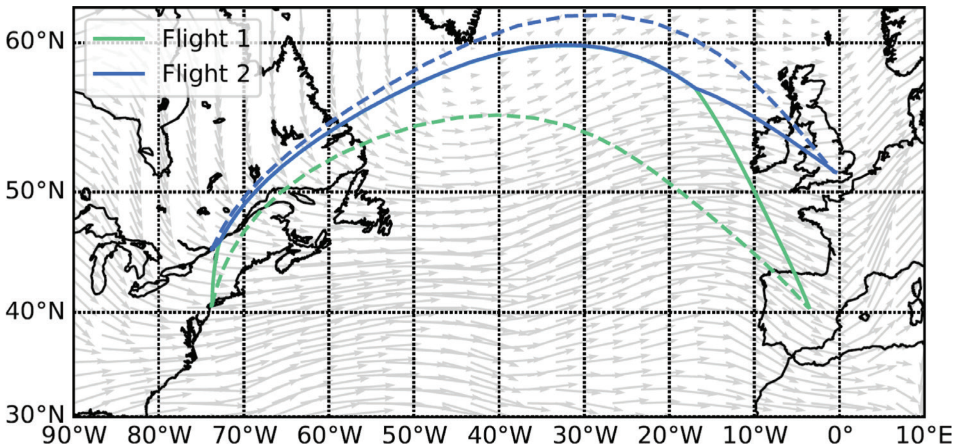

Fig. 7.2. Experiment A: State variables.

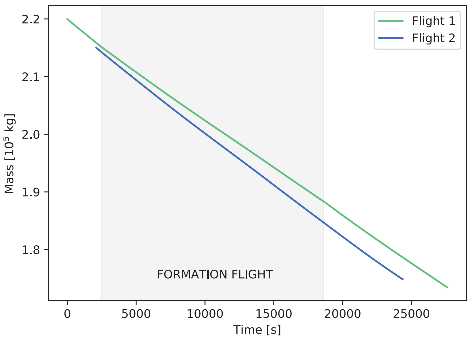

(a) Mass

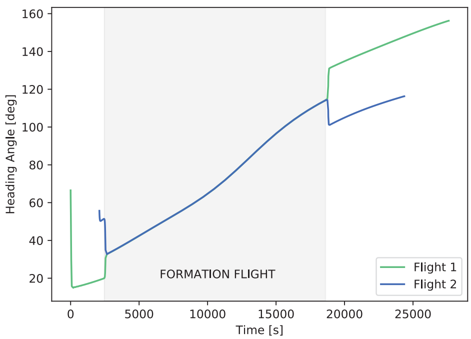

(b) Heading angle

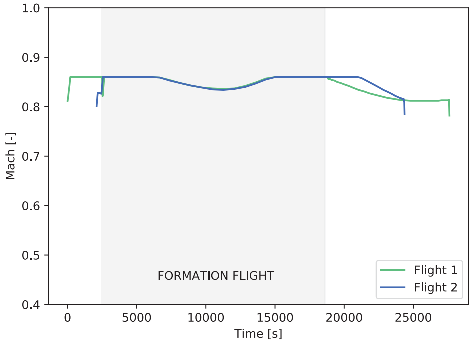

(c) Mach number

Fig. 7.3. Experiment A: Control variables.

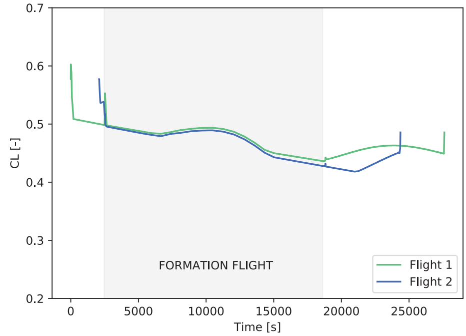

(a) Lift coefficient

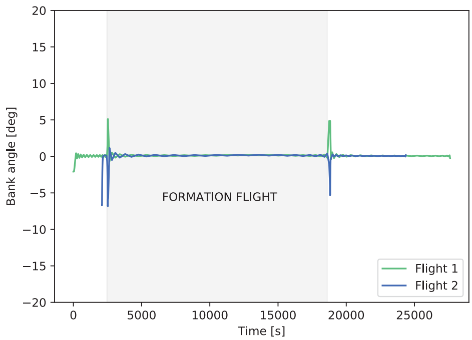

(b) Bank angle

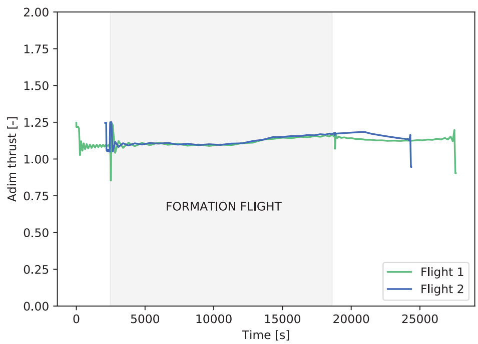

(c) Adimensional thrust

All the state variables vary smoothly, except the heading angle and the Mach number at the beginning and at the end of the flight. This behavior of the state variables is typical in boundary value problems, in which a quick maneuver is necessary to steer each aircraft from its initial state to its optimal route and from the optimal route to the final state. On the other hand, the control variables vary in a quite smooth way except around the switching instants. Notice that, the Gibbs phenomenon, described in Section 5.3.2, is present near the rendezvous and the splitting locations. However, this non-smooth behavior at the switching times lasts for a very short period of time compared with the total flight time.

Table 7.2. Experiment A: Solo and formation flight results for Flight 1.

	Flight Time [h]	Fuel Burn [kg]	Covered Distance [km]	DOC [mu]
Formation F.	7.68	46543.93	6716.44	40875.15
Solo F.	7.47	48596.82	6205.81	42085.37

Table 7.3. Experiment A: Solo and formation flight results for Flight 2.

	Flight Time [h]	Fuel Burn [kg]	Covered Distance [km]	DOC [mu]
Formation F.	16.9	40130.77	5348.58	34776.74
Solo F.	6.18	30683.14	5462.84	34452.60

In this experiment, the great circle distance between departure and arrival locations of Flight 1 is 5761.08 km and the great circle distance between departure and arrival locations of Flight 2 is 5214.72 km. For these flights, the great circle distance between departure locations is 537.00 km and the great circle distance between arrival locations is 1244.77 km. Thus, this scenario and the selected fuel burn saving for the trailing aircraft can be considered not optimistic for formation flight.

Comparison with the results obtained in solo flight

Tables 7.2 and 7.3 summarize the results obtained in formation and solo flights for Flight 1 and Flight 2, respectively. As expected, the flight times increase for both aircraft in formation flight with respect to solo flight, although for Flight 2 this flight time increment is negligible. Moreover, the fuel consumption of Aircraft 2, the leader aircraft, increases whereas the fuel consumption of Aircraft 1, the trailing one, decreases. The DOC is expressed in generic monetary units, mu. The total DOC of formation flight is almost one thousand generic monetary units lower than that of the solo flight, which amounts to more than one percent of reduction. For Flight 1, the total flight distance covered in formation flight is more than 500 km larger than in solo flight. Surprisingly, for Flight 2, the total flight distance covered in formation flight is smaller than the distance covered in solo flight. Obviously, both of them are higher than the great circle distance. The reason behind this unexpected result for Flight 2 is the Jet Stream. Indeed, in order to get the greatest benefits from the wind field, Aircraft 2 in solo flight takes a route more than 200 km longer than the orthodromic route. In case of formation, this large detour, which would involve both aircraft, becomes less advantageous and therefore it does not appear in the optimal solution.

7.3. Experiment B: Two-Aircraft transoceanic mission design with delays in the departure times

7.3.1. Description of the experiment

The flights considered in Experiment B, Flight 1 and Flight 2, have the same departure and arrival locations, the same boundary values for the state variables of each aircraft, and the same fuel burn savings for the trailing aircraft as in Experiment A. As before, in case of formation flight, Aircraft 1, associated to Flight 1, is forced to be the trailing aircraft and Aircraft 2, associated to Flight 2, is the leader one. The difference with respect to Experiment

A is that several delays in the departure times of both flights have been considered.

This experiment has been carried out to determine how delays in the departure times of both flights affect the formation flight, in terms of routes, rendezvous and splitting locations and times, until formation flight becomes non-optimal and, as a consequence, solo flights are selected by the algorithm.

Table 7.4. Experiment B: Delays in the departure time with respect to the baseline scenario for the different cases.

	Delays [min]	
Cases	Flight 1	Flight 2
B_1	20	0
B_2	15	0
B_3	10	0
B_4	5	0
B_5	-	-
B_6	0	5
B_7	0	10
B_8	0	15
B_9	0	20
B_{10}	0	25

For this analysis, several numerical simulations have been conducted introducing delays in the departure times of both flights in Experiment A, namely, 10:15 for Flight 1 and 10:50 for Flight 2, which represents the baseline case. In particular, five-minute increments in the delays have been considered for each flight. The actual values of the delays are listed in Table 7.4, in which each case is identified by a different symbol B_1 ,...,B_{10}, being $B5$ the baseline case.

7.3.2. Results

Optimal routes

For a better understanding of the results, the optimal aircraft routes obtained for different delays in the departure times are represented together in Fig. 7.4, in which the green and blue lines represent the optimal routes of Flight 1 and Flight 2, respectively. The optimal route obtained in the baseline case, B_5, is represented with a thicker line. Notice that, in this figure, the scale is not the same for latitude and longitude axes, and the symbols on the third axis denote the different cases.

Optimal rendezvous and splitting locations and times

In particular, Fig. 7.4 shows the rendezvous and splitting locations for each case, which are represented with small black stars and triangles, respectively. It can be observed that there is a great dependency of the location of the rendezvous points on the delay. For instance, in cases B_6 and B_7, the rendezvous location is very close to the departure location of Flight 2. On the contrary, the splitting locations barely change with delay. When the delay on one departure time increases, since it takes more time for the delayed aircraft to reach the other one, the rendezvous point changes. However, once the formation is created, both aircraft follow a very similar route for all the cases regardless of the delay in the departure time, and therefore, the optimal splitting locations do not change significantly. In Table 7.5, the rendezvous and splitting locations and the distance covered flying in formation obtained in cases B_2,...,B_9 are displayed. Notice the proximity of the splitting locations in all the cases and the closeness among the rendezvous locations in cases B_6 and B_7 and the departure location of Flight 2. On the contrary, the individual flight times and the duration of the formation flight, as well as the rendezvous and splitting times significantly change due to the initial detour made by both aircraft to create the formation. In Table 7.6, the rendezvous and splitting times and the duration of the formation flight for each case are listed. Notice that in cases B_1 and B_{10} solo flight is the optimal option. Therefore, the corresponding results have not been reported in tables and figures, where only the results obtained in formation flight are given. Further information on the results of cases B_1 and B_{10} can be found in the results of Experiment A.

Fig. 7.4. Experiment B: Routes obtained in the different cases considered.

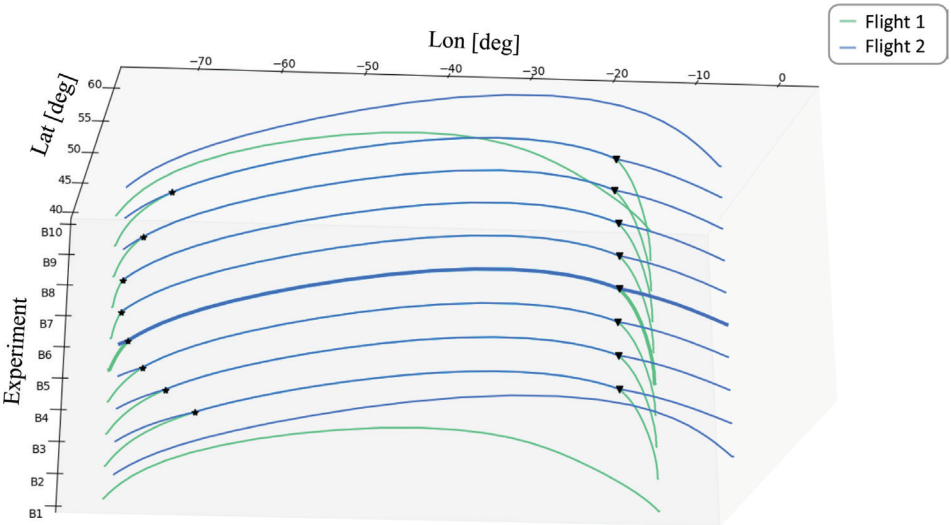

Table 7.5. Experiment B: Rendezvous and splitting locations and formation flight distance.

	Rendezvous (Lat, Lon) [*deg*]	Splitting (Lat, Lon) [*deg*]	FF Distance [*km*]
B_2	(51.26, −65.69)	(57.05, −17.13)	3208.86
B_3	(49.15, −68.85)	(57.04, −17.11)	3536.29
B_4	(47.10,−71.22)	(57.04, −17.06)	3829.61
B_5	**(46.04, −72.86)**	**(57.05, −16.83)**	**4024.45**
B_6	(45.48, −73.71)	(57.06, −16.71)	4130.80
B_7	(45.49, −73.72)	(57.06, −16.71)	4130.68
B_8	(47.59, −71.91)	(57.06, −16.69)	3823.66
B_9	(49.92, −69.09)	(57.06, −16.73)	3523.89

Table 7.6. Experiment B: Rendezvous and splitting times and formation flight duration.

	Time [*h*]		
	Rendezvous	Splitting	FF duration
B_2	1.58	5.21	3.63
B_3	1.22	5.21	3.99
B_4	0.90	5.22	4.33
B_5	**0.70**	**5.24**	**4.54**
B_6	0.67	5.32	4.66
B_7	0.75	5.40	4.66
B_8	1.15	5.45	4.30
B_9	1.61	5.58	3.96

Direct operating costs

The main results in terms of the objective functional are reported in Table 7.7. In particular, the variations in the flight time and in the fuel consumption for each flight and the reduction in the DOC obtained in cases B_2 ,...,B_9, all of them compared to solo flights results, are reported. It can be observed that, in general, the more the flight time of Flight 1 increases, the less the flight time of Flight 2 does and vice versa. Additionally, for those cases in which Flight 2 is delayed, the flight time increment of Flight 2 is very small. About the fuel burn, it can be seen that the greatest benefits for the trailing aircraft are achieved in the baseline case, which is the optimal one, as established in Experiment A. Notice the similarity among increments in fuel burn for Flight 2 in the results of cases B_6, B_7, B_8, and B_9, in which Flight 2 has a delay in the departure time. The greatest DOC reduction is 1.17% and the smallest is 0.02%. This tiny DOC reduction implies that flying in formation in case B_9 has negligible benefits, which could be further reduced by any contingency during the flight.

In general, one may conclude that the greatest flight distances covered in formation flight correspond to the highest total benefits in the fuel burn reduction. However, comparing the results displayed in tables 7.5 and 7.7, it is easy to check that longer distances covered in formation flight and greater duration of formation flight do not always imply more benefits in terms of reduction of DOC. It can be seen in tables 7.5 and 7.6, that in the results of cases B_6 and B_7, aircraft are flying 4.66 hours and about 4130 km in formation, being the greatest duration of formation flights and the greatest distance covered in formation flights, respectively. Nevertheless, as it can be observed in Table 7.7, the corresponding reductions in the DOC with respect to solo flights are 1.09% and 0.79%, respectively. The reduction of the DOC is slightly smaller than the one obtained in the baseline case, which amounts to 1.17%.

Table 7.7. Experiment B: Flight times, fuel burn and DOC variations compared to solo flights.

	△ Time [%]		△ Fuel burn [%]		
	Flight 1	Flight 2	Flight 1	Flight 2	△ DOC [%]
B_2	+2.56	+ 3.96	−3.30	+ 1.97	−0.14
B_3	+2.56	+ 2.60	−3.74	+ 1.80	−0.51
B_4	+2.57	+ 1.26	−4.13	+ 1.55	−0.89
B_5	**+2.79**	**+ 0.05**	**−4.22**	**+ 1.13**	**−1.17**
B_6	+3.79	+ 0.14	−4.15	+ 1.01	−1.09
B_7	+4.94	+ 0.13	−3.74	+ 1.01	−0.79
B_8	+6.07	+ 0.08	−3.06	+ 1.01	−0.36
B_9	+7.25	+ 0.07	−2.54	+ 1.00	−0.02

Table 7.8 has been added to give information about the total detour done by each flight. As in Experiment A, in all the cases considered in Experiment B there is a reduction in the distance covered by Flight 2 in formation flight compared to solo flight. Noteworthy is the great detour made by Flight 1 in the formation flight solution: about 500 kilometers of diversion from the solo flight route.

Table 7.8. Experiment B: Extra distance covered compared to solo flight distance.

	△ Distance [*km*]	
	Flight 1	Flight 2
B_2	451.21	−123.32
B_3	455.03	−127.23
B_4	467.05	−123.25
B_5	**510.62**	**−114.26**
B_6	543.56	−108.73
B_7	544.79	−111.76
B_8	516.48	−110.18
B_9	507.60	−109.73

Computational time

Computational times have been quantified in order to show the advantages in terms of computational time to solve the formation mission design problem given by the method presented in this thesis with respect the multiphase approach. The same instances of the problem have been solved with both techniques.

The average computational time to find the solution has been 15.234 s. For the sake of comparison, the same problem has been solved using a multiphase method [Hartjes et al., 2019]. In this case, two different OCP have been solved, namely, one in which aircraft flight solo and another one in which they are forced to fly in formation. The average computational time has been 7.784 s.

7.4. Experiment C: Three-aircraft transoceanic mission design with different fuel savings schemes

7.4.1. Description of the experiment

Experiment C involves three transoceanic eastbound flights, Flight 1, Flight 2 and Flight 3, with given fuel savings scheme and boundary values of the state variables. Flight 1, Flight 2, and Flight 3 are operated by Aircraft 1, Aircraft 2, and Aircraft 3, respectively. The three flights considered in this experiment have the following departure and arrival locations, the first two of them being the same as in Experiment A:

- Flight 1: New York (JFK) - Madrid (MAD).
- Flight 2: Montreal (YUL) - London (LHR).
- Flight 3: Boston (BOS) - Paris (CDG).

The departure times of Flights 1,2, and 3, are set to 10:15, 10:50, and 10:30, respectively. The first two of them are the same as in Experiment A. The boundary conditions for the state variables of the three aircraft are given in Table 7.9. The boundary conditions for the state variables of Aircraft 1 and Aircraft 2 are the same as in Experiment A.

Table 7.9. Experiment C: Boundary conditions for the three flights.

Symbol	Units	Flight 1	Flight 2	Flight 3
ϕ_I	[deg]	40.64	45.47	42.36
ϕ_F	[deg]	40.48	51.47	48.85
λ_I	[deg]	−73.78	−73.74	−71.06
λ_F	[deg]	−3.57	−0.45	2.35
χ_I	[deg]	66.51	55.70	56.46
V_I	[m/s]	240	240	240
V_F	[m/s]	220	220	220
m_I	[kg]	220 000	215 000	210 000

The relative position of each aircraft in the formation is selected in advance. In case of two-aircraft formation flights that include Aircraft 3, Aircraft 3 will be the leader aircraft and Aircraft 1 or Aircraft 2 will be the trailing. In case of two-aircraft formation flights that do not include Aircraft 3, Aircraft 2 will be the leader aircraft and Aircraft 1 will be the trailing. In case of three-aircraft formation flights, Aircraft 3 will be the leader aircraft, Aircraft 2 the intermediate, and Aircraft 1 the trailing.

Table 7.10 summarizes the results obtained assuming that each flight is performed as a solo flight. It can be observed that the flight times, the fuel consumption, the covered distance, and the DOC of each flight are quite different.

Table 7.10. Experiment C: Results for the three solo flights.

	Flight 1	Flight 2	Flight 3
Flight Time [*h*]	7.47	6.19	6.90
Fuel burn [*kg*]	48596.82	39683.14	42877.40
Covered Distance [*km*]	6205.81	5462.84	5945.89
DOC [*mu*]	42087.53	34462.32	37466.18

An analysis is performed to determine how the fuel savings scheme affects the formation flight, in terms of routes, rendezvous and splitting locations and times, and flight times.

As already mentioned, the only formation configuration allowed is the in-line formation and the relative position of the aircraft in the formation is fixed. The considered benefits for the intermediate and the trailing aircraft range from 6% to 14%. Several numerical simulations have been conducted introducing changes in the fuel savings for the intermediate and trailing aircraft, in which each case is identified by a different symbol $C_1,\ldots,C_5$. The fuel savings considered in the different cases for the intermediate and trailing aircraft have been listed in Table 7.11.

Table 7.11. Experiment C: Fuel savings for the intermediate and the trailing aircraft, in the different cases.

	Fuel savings [%]
C_1	6
C_2	8
C_3	10
C_4	12
C_5	14

7.4.2. Results

Optimal routes

The optimal formation flight routes obtained in case C_3 are represented in Fig. 7.5, together with the solo flight routes and the wind field. In this figure, dashed lines are used to plot solo flight routes and solid lines are used to represent formation flight routes. Green, blue, and red lines represent Flight 1, Flight 2, and Flight 3, respectively. For the sake of brevity, the routes obtained in the other cases have been omitted.

Fig. 7.5. Experiment C: Solo and formation flight routes.

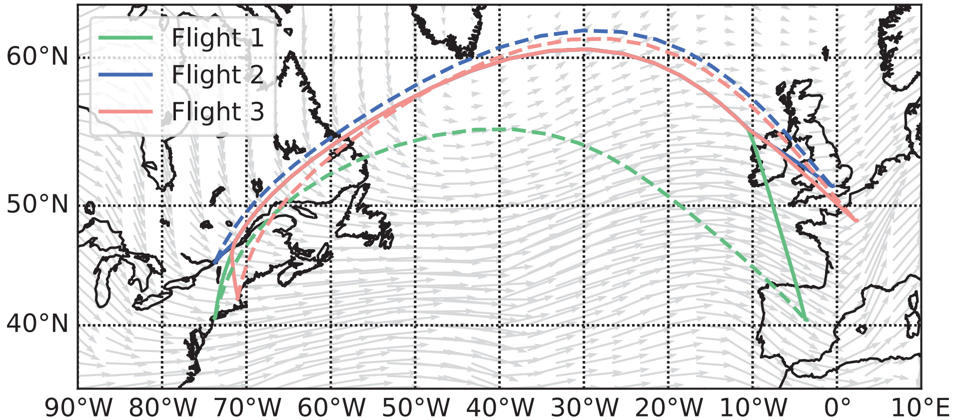

In the optimal solutions of all the cases considered, there are five discrete states of the switched dynamical system that represent the joint behavior of the aircraft. In Fig. 7.6 a schematic representation of these five discrete states, from State I to State V, is given. In particular, each discrete state is characterized by the following modes

- State I: all the aircraft fly in solo mode.
- State II: two aircraft fly in formation and one in solo mode.
- State III: all the aircraft fly in formation.
- State IV: two aircraft fly in formation and one in solo mode.
- State V: all the aircraft fly in solo mode.

Fig. 7.6. Experiment C: Discrete states representation for three-aircraft formation.

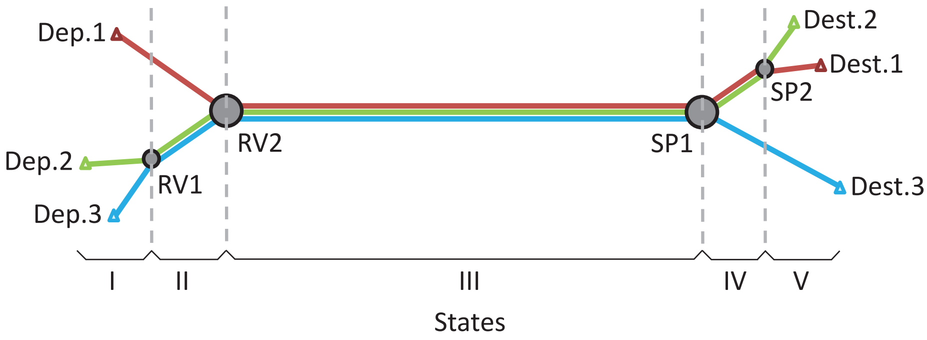

It is easy to see that in the switches among these discrete states, there are two rendezvous points, RV1 and RV2, where RV1 is the first one and RV2 is the second one, and two splitting points, SP1 and SP2 , where SP1 is the first one and SP2 is the second one. In Fig. 7.6, the points RV1, RV2, SP1, and SP2 are represented with grey points. Small triangles have been used to represent the departure and destination of each flight.

Optimal rendezvous and splitting locations and times

Figs. 7.7 and 7.8 represent the three-aircraft routes obtained in cases C_1,...,C_5. In these figures, the behavior of the rendezvous and splitting locations, respectively, is detailed. It can be observed that the location of both rendezvous points, RV1 and RV2, and the location of the second splitting point, SP2, do not present significant variations in the different cases. On the contrary, the location of the first splitting point, SP1, notably changes, differing in some cases in more than 1000 km. This variation in the location of SP1, which is the point in which there is a switch between State III and State IV, implies that the three-aircraft formation time and distance largely depend on the fuel savings scheme. Consequently, the formation time and distance in State IV also have a high dependency on it. Results in tables 7.12 and 7.13 confirm this conclusion. It can also be observed in these tables that, in all the considered cases, the formation times and distances corresponding to discrete State II are small compared to other discrete states.

Fig. 7.7. Experiment C: Routes obtained in the different cases considered. Detail of the rendezvous locations.

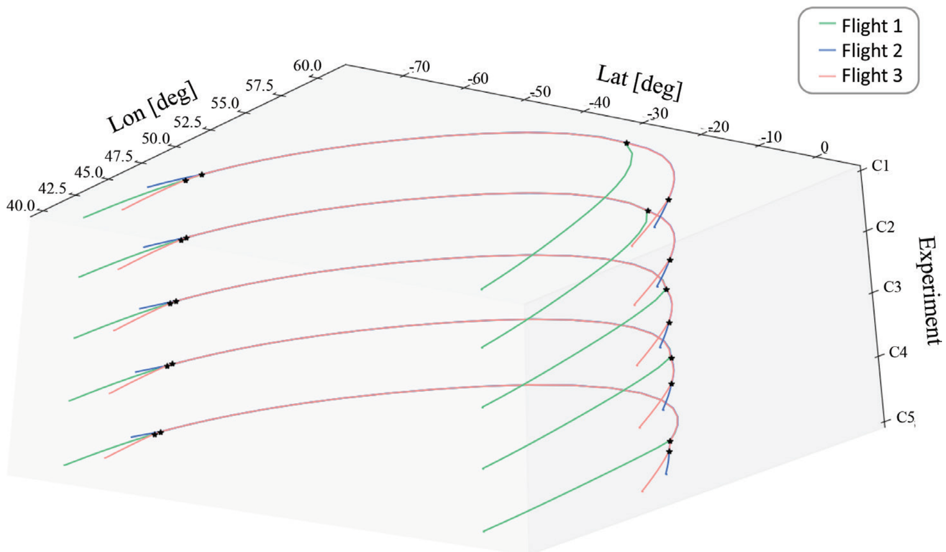

Fig. 7.8. Experiment C: Routes obtained in the different cases considered. Detail of the splitting locations.

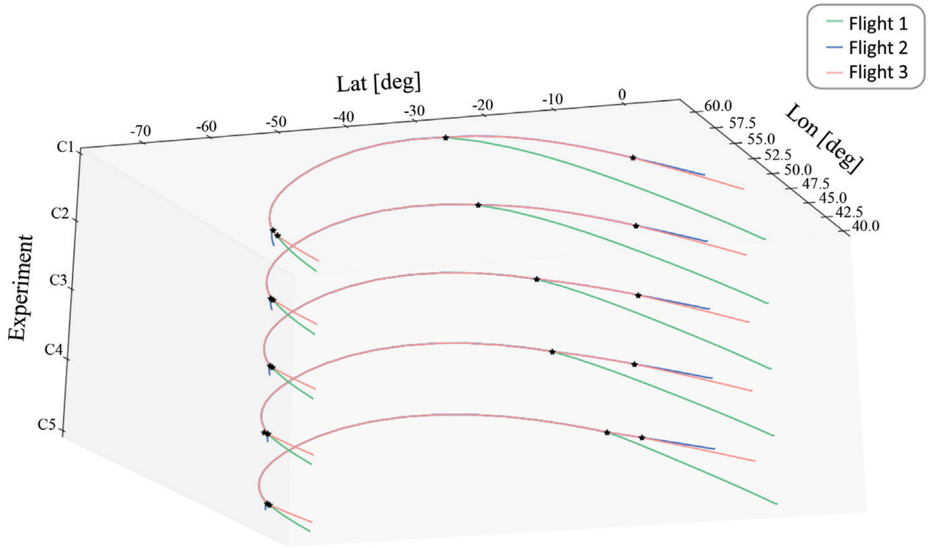

Table 7.12. Experiment C: Formation distances for the two- and three-aircraft formation phases.

	Formation distances [*km*]		
Cases	State II	State III	State IV
C_1	113.53	3008.99	1371.24
C_2	38.19	3323.62	1142.36
C_3	41.01	3743.05	737.69
C_4	44.48	3847.74	595.32
C_5	41.44	4229.41	257.29

Table 7.13. Experiment C: Formation times for the two- and three-aircraft formation phases.

Cases	Formation times [h]		
	State II	State III	State IV
C_1	0.13	3.30	1.72
C_2	0.06	3.69	1.43
C_3	0.05	4.26	0.92
C_4	0.04	4.42	0.84
C_5	0.06	4.92	0.74

Direct operating costs

The main results related to the objective functional obtained in Experiment C are reported in Table 7.14. In particular, the increase of the flight time of each flight, the reduction or increase of the fuel burn and the reduction in the DOC with respect to the results obtained assuming each flight is performed as a solo flight, are reported. It can be seen in this table that, for case C_5, the reduction in the DOC is almost 4% comparing to the case in which formation is not allowed.

Table 7.14. Experiment C: Total flight times, fuel burn and DOC reduction compared to solo flights, in the different cases.

	Δ Time [%]			Δ Fuel burn [%]			
	Flight 1	Flight 2	Flight 3	Flight 1	Flight 2	Flight 3	Δ DOC [%]
C_1	2.28	0.13	0.30	−1.83	−4.17	0.90	−1.14
C_2	2.45	−0.02	0.16	−2.87	−5.81	1.10	−1.80
C_3	2.89	−0.06	0.10	−4.15	−7.39	1.25	−2.51
C_4	2.90	−0.19	0.01	−5.29	−9.14	1.41	−3.25
C_5	3.54	−0.10	0.02	−6.69	−10.64	1.45	−3.97

Computational time

The average computational time to find the solution has been 15.274 s. For the sake of comparison, the same problem has been solved using a multi-phase method [Hartjes et al., 2019]. In this case, 13 different OCP have been solved, since, in this case, there are 13 possible flight phase sequencing options, as shown in [Hartjes et al., 2019]. The average computational time has been 90.948 s. This shows that the method presented in this thesis is able to drastically reduce the computational time to solve formation mission design problems.

7.5. Conclusions

The results of the numerical experiments described in this chapter show that delays and changes in the fuel savings scheme have significant influence on the formation mission. The results show that a reduction of, approximately, 1% and 4% in terms of the DOC can be achieved for two- and three- aircraft formations, respectively, compared to solo flights, in non-optimistic scenarios, as the ones selected in this chapter. The results demonstrate that the proposed method for formation mission design in the absence of uncertainties is fast, accurate and easily scalable. The average computational times to find the solution for two- and three- aircraft mission design problems using a common desktop computer have been around 4 and 15 seconds, respectively, which translates to one half and one sixth of the computational time required by the multiphase method, respectively.